Characterisation of solution annealed VT-14 titanium alloy using eddy current based electrical resistivity measurements

Article *in* Transactions of the Indian Institute of Metals · October 2010

DOI: 10.1007/s12666-010-0118-6

B. Sasi
Indira Gandhi Centre for Atomic Research

Purna Chandra Rao Bhagi
Indira Gandhi Centre for Atomic Research

Baldev Raj
Indira Gandhi Centre for Atomic Research

TP 2416

Transactions of The Indian Institute of Metals
Vol. 63, Issue 5, October 2010, pp. 773 - 777

Characterisation of solution annealed VT-14 titanium alloy using eddy current based electrical resistivity measurements

B. Sasi, B.P.C. Rao, T. Jayakumar and Baldev Raj

Non Destructive Evaluation Division, Indira Gandhi Center for Atomic Research, Kalpakkam–603 102, Tamil Nadu, India

E-mail: bpcrao@igcar.gov.in

Received 19 March 2010
Accepted 12 July 2010
Online at www.springerlink.com

***Keywords**:*
titanium alloy; eddy current; electrical resistivity; microstructure characterisation;

Abstract

This paper discusses characterisation of microstructures in Ti-4.5Al-3Mo-1V (VT-14) alloy specimens solutionized in the temperature range of 923K-1373K, using room temperature electrical resistivity measurements. Using phase angle of impedance change in eddy current coil as a parameter, calibration curve between resistivity and phase angle has been established using three reference specimens of known resistivity. The changes in the electrical resistivity of the specimens have been correlated with optical microscopy investigations. The electrical resistivity of unstable β phase has been compared with α and α′ phases and possible reasons for higher resistivity of β phase and lower resistivity of α′ have been given based on the rule of mixtures and scattering and mobility of electrons. The electrical resistivity of α′ martensite phase of the chosen VT-14 alloy has been determined as 1.04 αΩ-m. The studies reveal that it may be possible to identify the β transus temperature of α+β titanium alloys from the electrical resistivity data.

1. Introduction

Titanium alloys are widely used in aerospace, marine, refinery and nuclear processing and chemical industries in view of their excellent corrosion resistance and better intermediate temperature strength. Among the three types of titanium alloys i.e. α, β, α+β, the α+β alloys account for more than 60% of all titanium tonnage in the market and contain mixtures of α and β phases depending on the quantity of α and β stabilizers. The dual phase structure of these alloys makes them considerably stronger than either α or β alloys. Further, α+β alloys can be strengthened by heat treatment. To get desired mechanical properties, α+β alloys are usually heated close to the β transus temperature in α+β phase field and then (solutionizing) quenched followed by aging at a moderate temperature [1-2]. In any α+β titanium alloy, volume fraction of β phase increases with increase in solutionizing temperature upto β transus temperature. But as the amount of β stablising elements is fixed, the volume fraction of β stablising elements in β phase decrease with increase in temperature. Such a β phase composition upon quenching from the α+β phase field, is unstable at room temperatures at which the β phase decomposes by a martensitic type reaction forming either α′ (acicular, hcp) or α′′ (orthorhombic) phase depending on the solutionizing temperature and chemical composition of the alloy [3]. Heating above the β transus temperature would result in formation of β phase with unacceptable coarse grains. The phase transformation kinetics and microstructural changes in α+β alloy system during different heat treatment conditions have been well studied [4-5]. VT-14, i.e. Ti-4.5Al-3Mo-1V is a α+β type alloy. The microstructures and mechanical properties of heat treated VT-14 alloy depend on the volume fraction of primary α, unstable β and α′ (acicular) or α′′ (orthorhombic) phases. Thus characterisation of microstructural changes during the heat treatment of VT-14 alloy is important for ensuring of specific mechanical properties.

Nondestructive evaluation (NDE) based assessment of mechanical properties and characterisation of microstructures is very attractive [6]. NDE techniques enable on-line assessment of microstructures or mechanical properties in production line and can also be used on operating components e.g. for assessment of degradation in microstructure, corrosion and fatigue damage. Use of ultrasonic, eddy current (EC), non-linear ultrasonic, thermography, photo acoustic techniques and thermoelectric power measurements has been reported for assessment of microstructures, mechanical properties, plastic deformation and fatigue damage in titanium alloys [7-10]. NDE techniques are based on physical principles and in these techniques, the interaction of a medium (like electromagnetic radiation and sound waves) with various attributes present in a material are studied to establish a quantitative relationship between NDE parameters and a material attribute of interest. Ultrasonic techniques utilize the changes in attenuation and longitudinal or shear velocities while eddy current techniques use the change in electrical resistivity, ρ (1/electrical conductivity) and relative magnetic permeability, μ_r [11]. The electrical resistivity is measured nondestructively using two-point or four-point probe method or using eddy current technique. While the former methods are based on Ohm's law involving measurement of voltage drop between two electrodes separated by a fixed distance, the latter technique works on electromagnetic induction. According to the Mathiessen's rule [12], the electrical resistivity of the material, ρ_{total} is given by

$$\rho_{total} = \rho_t + \rho_i + \rho_d \quad (1)$$

where ρ_t, ρ_i and ρ_d represent the individual contributions of thermal vibrations, impurity and deformation, respectively. When thermal and deformation components are absent, impurities mainly disturb the periodic lattice and cause scattering of electrons. This reduces the mean free path of electrons between collisions and increases the electrical resistivity [13-14]. The two most important scatters in metals and alloys are phonons and impurities and the latter dominating at sufficiently low temperatures while electron-phonon component dominates at high temperatures. In the case of $\alpha+\beta$ titanium alloy, the electrical resistivity of the alloy is complex and depends on the volume fraction of α and β phases and can be expressed based on the rule of mixture [12] as

$$\rho_{\alpha+\beta} = \rho_\alpha V_\alpha + \rho_\beta V_\beta \quad (2)$$

where V_α and ρ_α are volume fraction and resistivity, respectively, of primary α phase and V_β and ρ_β are the volume fraction and resistivity, respectively, of unstable β phase. ρ_α and ρ_β depend on temperature and chemical composition especially the α and β stabilizing elements. The significant variations in resistivity values for different phases and changes with composition and temperature are expected to allow determination of transformation temperatures and kinetics. Several researchers used eddy current based electrical resistivity measurements to characterize microstructures in metallic materials [11,15].

Hagemaier [16] reported detection of hydride and alpha-case depth in titanium alloys using eddy current technique and determined the alpha case depth when it is greater than 12.5 µm. Rosen [17] used 'Sigmatester device' for electrical conductivity measurement to evaluate the effect of high temperature exposure on the mechanical properties of the Ti-6Al-4V alloy and showed good correlation between fracture strength and electrical resistivity. Veeraraghavan et al. studied the phase transformation in Ti- (25-52) at.% Al alloys by using two-point probe electrical resistivity measurements at high temperature and reported that the α and β phases have distinctly different resistivity and temperature dependencies [18]. Fabien et al. studied the phase transformations in Ti-17 alloy during heat treatment and estimated the volume fraction of α phase at high temperature using X-ray diffraction (XRD) technique and measured the electrical resistivity using four-point probe method. They reported good correlation between volume fraction of α phase at high temperature and electrical resistivity [4]. Collins and Gehlen [19] reported variations in magnetic susceptibility of pure Ti, disordered (α) Ti-Al (2-15% Al) and ordered (α_2) Ti_3Al in the temperature range of 74-400K. Studies on electrical resistivity measurements on VT-14 alloy using eddy current technique and their correlation to heat treated microstructures are scarce.

The objective of the present study is characterisation of microstructural changes in solutionized VT-14 alloy specimens using eddy current based electrical resistivity measurements. This paper gives details of heat treatment and experimental set up used for room temperature resistivity measurements and then discusses the results of specimens solutionized at different temperatures. The paper attempts to explain using the rule of mixers and electron scattering, how electrical resistivity of VT-14 alloy varies with the contributions of primary α and unstable β or α' martensite phases present in the microstructures in specimens heat treated at different solutionizing temperatures and then points out how resistivity measurements can be used to identify the β transus temperature of $\alpha+\beta$ titanium alloys.

2. Material and eddy current test procedure

2.1 Material and heat treatment condition

The specimens used in the present study are made of titanium alloy VT-14 (Ti-4.5Al-3Mo-1V) of dimension 20x20x12 mm^3 from a β heat treated (1323K/1h) and water quenched block of 12 mm thickness. These specimens are subjected to solutionizing treatment in the temperature range of 923K-373K at an interval of 50K for 1h followed by water quenching. Metallographic examination is carried out to reveal microstructure in different specimens. The etchant used is Kroller's reagent.

2.2 Principle of eddy current technique

Eddy current technique works on the principle of electromagnetic induction. An alternating current (frequency in the range of 50 Hz – 5 MHz) is made to flow in a probe coil which in turn produces an alternating magnetic field around it. When the probe coil is brought close to an electrically conducting material, eddy currents are induced in the material. These eddy currents are parallel to the direction of probe coil winding as shown in Fig. 1. The eddy currents also produce magnetic fields (secondary). The primary and the secondary magnetic fields are always opposite to each other as a result, there will be a small change in probe coil impedance (a few micro ohms) which can be measured using sensitive bridge circuits [11]. The change in probe coil impedance depends on variations in the following:

- ***electrical resistivity (ρ)*** in nonmagnetic materials such as stainless steel, titanium, aluminum etc.
- ***relative magnetic permeability (μ_r)*** in magnetic materials such as carbon steel, Maraging steel.

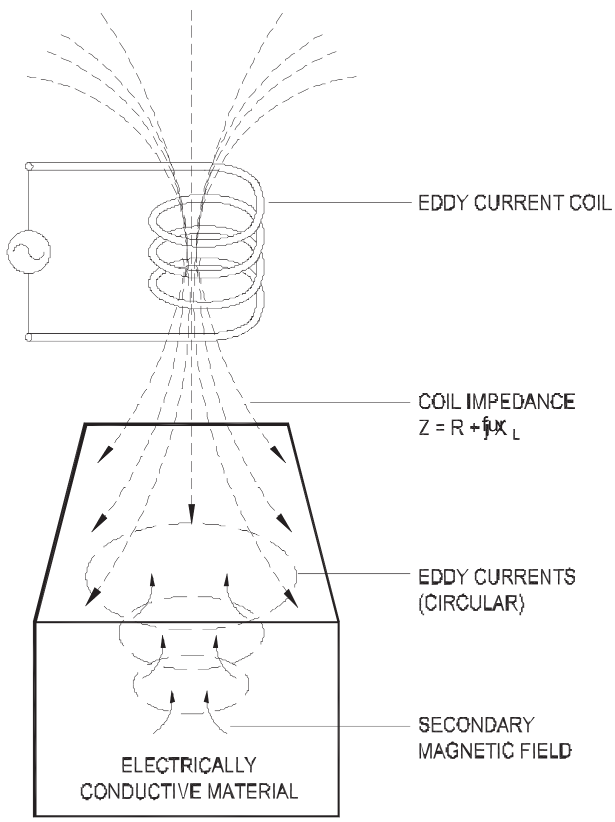

Fig. 1 : Principle of eddy current technique.

- ***microstructure*** due to changes in chemical composition, heat treatment, forming procedure and grain size etc. which in turn change ρ and μ_r.
- ***coil excitation frequency (f)*** which governs the depth of interrogation (δ) following the classical *skin-effect* phenomenon viz. $\delta = 50/\sqrt{\rho / f\mu_r}$, mm, where ρ is in µ&!-cm and f is in Hz and μ_r relative permeability is constant (1 for non-ferromagnetic materials).
- ***lift-off*** which is the distance between probe coil and specimen surface.

Presence of any discontinuities in the material such as cracks, corrosion, wall thinning, inclusion and others that alter ρ and μ_r causes distortion to eddy current flow and in turn, changes the probe coil impedance which is a complex quantity with resistance (R) and reactance (X_L) components. The locus of impedance change during the movement of a probe coil over the material surface is called an EC signal [11]. The magnitude of EC signal provides information about the severity of the discontinuity while the phase angle with respect to lift-off provides information about the depth and location of the discontinuity. Phase angle of EC signal is effectively used in eddy current technique to discriminate desired discontinuity from an undesired discontinuity or noise [11,20]. In the present study, phase angle information of EC signal is utilised for determination of ρ. The change in probe coil impedance due to change in ρ is analysed because VT-14 is a non-magnetic alloy and there is no influence expected from μ_r. As seen from Fig. 2, when a probe coil is brought from infinity and placed on a non-magnetic material, the impedance curve changes from 'air' to a definite position in the fourth quadrant while the curves change from 'air' to different positions in the first quadrant for magnetic materials.

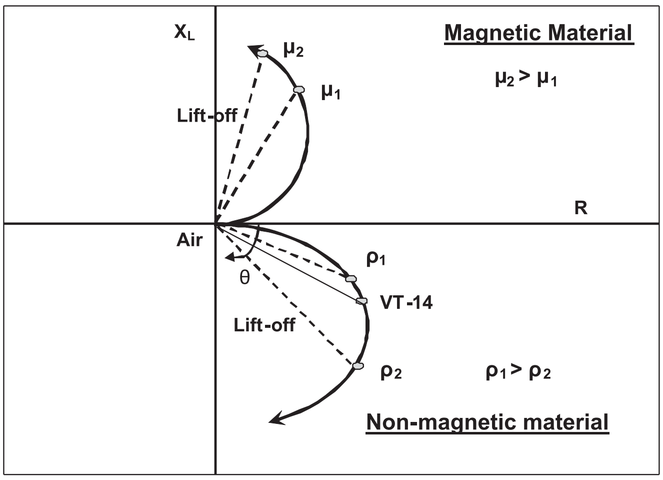

Fig. 2 : Response on the impedance plane for different metallic materials.

2.3 Experimental measurements

The changes in coil impedance are measured using an eddy current instrument (Model ECT 3100) with an absolute surface probe of 5 mm diameter. The excitation frequency is optimised at 150 kHz to achieve good phase angle separation between resistivity variations and to avoid the influence of thickness changes on resistivity measurements as the eddy currents almost vanish beyond 3.5 mm depth (3δ) at this frequency. As change in phase angle due to variation in electrical resistivity of materials is comparatively more than the magnitude for the VT-14 alloy specimens, phase angle has been used as a parameter. During the measurements, a uniform and near zero lift-off is usually maintained to minimize lift-off related errors.

In order to determine small changes in room temperature electrical resistivity in specimens subjected to different solutionizing temperatures, a calibration graph between ρ and θ (in degree) is generated. As the expected change in ρ is in the range of 1.0 and 2.0 $\mu\Omega$-m, three well characterised standard reference specimens having known electrical resistivity in this range (Hastalloy X - 1.15 $\mu\Omega$-m, Hastalloy B - 1.33 $\mu\Omega$-m, Ti-6Al-4V - 1.72 $\mu\Omega$-m) have been used. The phase angle (angle between positive horizontal axis and the lift-off axis) of the impedance curve is measured after aligning the phase angle of impedance curve of Hastalloy X at 0.79 radians (45°) for convenience. Thus, when resistivity of specimens is higher than that of Hastalloy X, the phase angle will be less than 0.79 radians and vice versa.

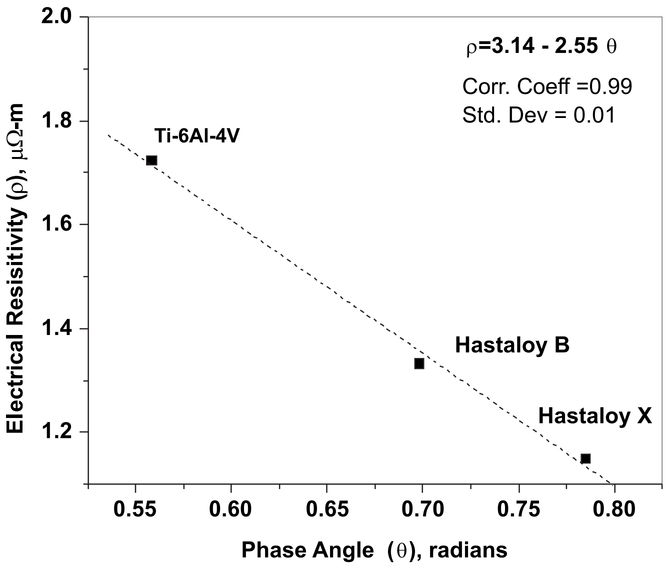

Fig. 3 : The calibration curve between measured phase angle of impedance curve and electrical resistivity of standard reference specimens.

The probe coil is placed on standard reference specimens and the real and imaginary components of the impedance changes are digitised 50 times using a 12-bit analogue-to-digital converter (ADC) card and the average data are stored. From this data, phase angle of the impedance curve (extreme point denoting probe coil on specimen) is determined and the calibration graph shown in Fig. 3 with the following quadratic equation yielding a correlation coefficient of 0.99 has been obtained:

$$\rho = 3.14 - 2.55\theta \ \mu\Omega - m \qquad (3)$$

The room temperature electrical resistivity of specimens at different solutionizing temperature is calculated by substituting the measured phase angle value in equation (3) with a scatter of ±0.005 radians. In order to understand the changes in microstructure and to correlate with electrical resistivity changes, optical microscopy has been carried out on solutionized VT-14 alloy specimens.

3. Results and discussion

Figure 4 shows the optical micrographs of specimens solutionized at 1073K, 1123K, 1173K and 1273K. As can be

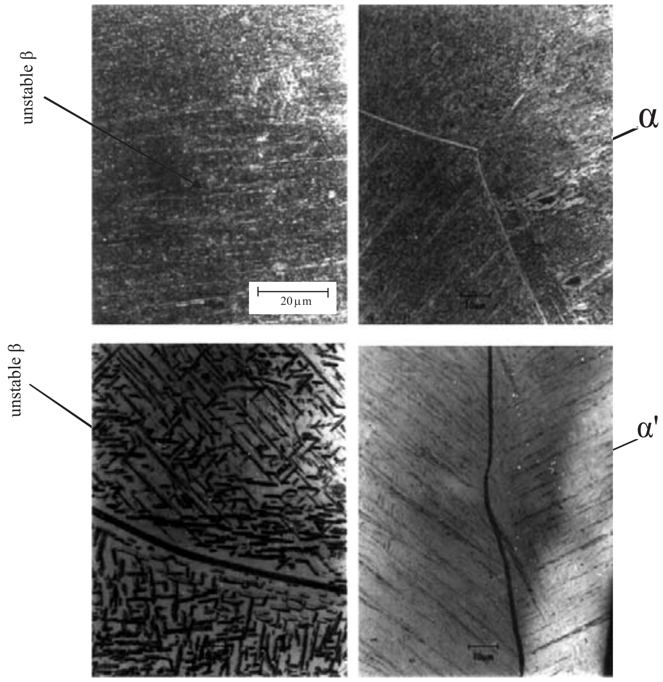

Fig. 4 : Micrographs of VT-14 alloy specimen solutionized at a)1073K, b) 1123K has primary α (black) in unstable β phase(white), c) at 1173K has primary α (black) in α′ martensite phase and (d)1273K has only α′ martensite phase.

seen from Fig. 4a, at 1073K, unstable β phase (bcc) is present in primary α phase (dark) regions. The amount of primary α phase (hcp) is found to decrease in specimen solutionized at 1123K (refer Fig. 4b) with a corresponding increase in amount of unstable β phase(white). Increase in unstable β phase is due to decrease in atom percentage of β stabilizing elements upto β transus temperature which is clearly above 1123K. In specimen solutionized at 1173K, presence of needle like α′ martensite phase is found in the primary α phase (dark) as shown in Fig. 4c. As expected this is due to the diffusionless transformation of unstable β phase to α′ martensite. The specimen solutionized at 1273K shows 100% α′ phase as shown in Fig. 4d indicating completion of the martensitic transformation beyond 1273K.

Figure 5 shows the impedance curves observed when the EC probe coil is placed on specimens solutionized at different temperatures. As can be noted, for the specimens solutionized at 923K, 1073K and 1123K, the curves moved up towards the Ti-6Al-4V standard reference specimen while for specimen solutionized at 1173K, 1223K, 1273K,1323K and 1373K, the curves moved down towards the Hastalloy B standard reference specimen. The upward and downward movement of the impedance curves with respect to the standard reference Hastalloy B correspond to increase and decrease in electrical resistivity respectively, in line with the discussion of Fig. 2. Electrical resistivity of specimens as a function of the solutionizing temperature is shown in Figure 6. As can be seen, an increase in the electrical resistivity is observed between 923K and 1123K, followed by a drastic decrease in resistivity upto 1273K and then becoming constant beyond 1273K. This overall trend is identical to the ultrasonic attenuation reported by Anish et al. [8] with soft unstable β phase having highest damping showing the maximum attenuation at 1123K and instead hard α′ martensite phase showing the lowest attenuation.

The initial increase in electrical resistivity up to 1123K is attributed to decrease in primary α phase and associated increase in volume fraction of unstable β phase with increase in solutionizing temperature, while the resistivity of both α and β phases is expected to increase following equation (1) due to increase in impurities in both α and β phases that increase the electron scattering. However, the volume fraction of α phase decreases with increasing solutionizing temperature while volume fraction of β phase increases. The volume fraction of β phase becomes almost 1 around 1123K. Thus, following the rule of mixers for resistivity of primary α and unstable β phases given in equation (2), it can be inferred that the electrical resistivity of unstable β phase is higher than that of the primary α phase, because the resistivity of the alloy increases with increase in volume fraction of unstable β phase. The observation of increase in resistivity upto 1173K is in agreement with that reported by Tarin et al. [21].

The drastic decrease in electrical resistivity observed during 1123K - 1273K is attributed to transformation of unstable β phase to α′ martensite phase (Fig. 4c). The resistivity is found to decrease with increase in solutionizing temperature upto 1273K due to increase in volume fraction of α′ martensite phase and corresponding decrease in primary α phase. The resistivity of the alloy is found to be constant after 1273K due to the presence of only α′ martensite phase as evident in Fig. 4d. Using this microscopy evidence of 100% formation of α′ phase, it is possible to determine the electrical resistivity of α′ martensite phase of the chosen alloy as 1.04 $\mu\Omega$-m.

The electrical resistivity data of α′ martensite phase can be given as an input parameter along with alloy composition and heat-treatment temperature for training artificial neural network proposed by Reddy et al. [22] for estimating the beta-approach curve and the β transus temperature based on β phase volume percentage. The lower resistivity of single and homogenous α′ martensite phase is attributed to decrease in impurities and electron scattering and thus results increase in the mean free path and the mobility of electrons. The lower resistivity of α′ phase must be valid for all α+β titanium alloys. For these alloys, it can be consolidated that increase in β stabilizing elements (also α stabilizing elements) lowers the β transus temperature and increases the volume fraction of α′ martensite phase upon quenching and is characterized by lower electrical resistivity. The resistivity of unstable β phase is expected to be higher than that of the α and α′ phases due to comparatively higher amount of impurities.

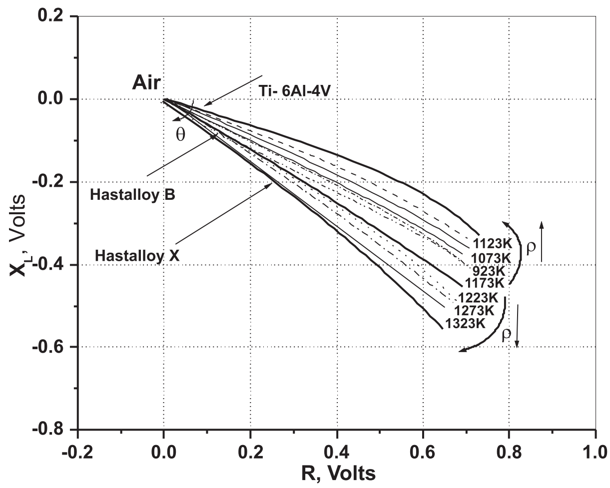

Fig. 5 : EC probe coil impedance curves observed for VT-14 alloy specimens at different solutionizing temperatures.

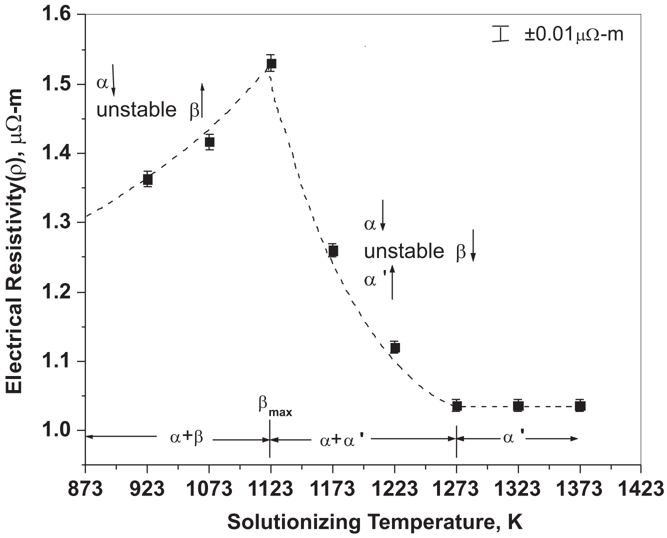

Fig. 6 : Variation in electrical resistivity with solutionizing temperatures.

4. Conclusion

Room temperature electrical resistivity of VT-14 alloy specimens solutionized in the temperature range of 923K-1373K for 1 hour and water quenched, has been measured at room temperature non-destructively using eddy current method. Phase angle of impedance change in eddy current coil is used as a parameter to establish a calibration curve between phase angle and electrical resistivity of three known reference specimens in the resistivity range of 1.15-1.72 $\mu\Omega$-m. The major conclusions arising from the study are as follows:

- Electrical resistivity of the VT-14 alloy is found to increase in the range of 923-1123K due to reduction in primary α phase and increase in volume fraction of unstable β phase and also due to higher resistivity of unstable β phase than that of primary α phase.
- Electrical resistivity is found to decrease in the range of 1123-1273K due to formation and increase in volume fraction of α′ martensite phase.
- 100% transformation of α′ martensite phase beyond 1273K is marked by a lowest and constant electrical resistivity of 1.04 μΩ-m, for the chosen VT-14 alloy.
- Electrical resistivity of unstable β phase is found to be higher than α and α′ phases. This is due to the presence of impurities which increase scattering of electron as a result of reduction in the mean free path for collision and the mobility of electrons.
- Electrical resistivity of α′ martensite phase is lower. This is attributed to be due to the decrease in impurities in homogenous α′ martensite phase reducing electron scattering and increasing the mean free path as well as mobility of electrons.
- The trend of electrical resistivity variations with increasing solutionizing temperature compares well with that of ultrasonic attenuation.
- As the α+β type titanium alloys are expected to exhibit constant lower electrical resistivity at temperatures above the β transus temperature, it may be possible to use the electrical resistivity data for determining the β transus temperature.

Acknowledgements

Authors thank Dr. Anish Kumar, NDE Division, IGCAR for many useful discussions.

References

1. Reed-Hill T E and Abbaschian R, *Physical Metallurgy principles*, third ed., Thomson Asia Pte. Ltd., Singapore, (2003).
2. Collings E W, Enderby J E, Gegel H L and Ho J C, Some relationship between the electronic and mechanical property of Ti Alloys, Discussed from the standpoint of fundamental alloy theory, in: Jaffee R J, Burte H M (Eds.), Titanium science and technology, Plenum Press, New York, **2** (1973) 801.
3. Moiseyev V N and Glasunov G, Titanium Alloys: Russian Aircraft and Aerospace Applications, Taylor & Francis, London, (2003).
4. Fabian B, Aeby-Gautier E, Geandier G, Teixeira J D, Appolaire B, Weishecker P and Anthony M, *Mater. Sci. Eng. A*, **476** (2008) 60.
5. Ahmed T, *Mater. Sci. Eng. A*, **243** (1998) 206-211.
6. Jayakumar T, Microstructural characterisation in metallic materials using ultrasonic and magnetic methods, PhD Thesis, University of Saarland, Saarbruecken, Germany; (1996).
7. Baldev Raj, Jayakumar T and Anish Kumar, *Trans. of the Indian Institute of Metals,* **57**(1) (2004) 13.
8. Anish Kumar, Jayakumar T, Baldev Raj and Ray K K, *Mater. Sci. Eng. A,* **360** (2003) 58.
9. Hector Carreon, *NDT&E Int.* **39** (2006) 433.
10. Vary A and Hull D R, *Mater. Eval.,* **43**(3) (1984) 3094.
11. Rao B P C, Introduction to Eddy Current Testing, in: Baldev Raj, Venkatraman B, (Eds.), Practical Eddy Current Testing, Narosa Publishing House, India, (2007).
12. Callister W D, Material Science and Engineering- An introduction, fifth ed., John Wiley & Sons, Inc, New York, (1999) 651.
13. Azaroff L V, Introduction to Solids, TMH Publishing Company Ltd., India, (1977) 247.
14. Dekker A J, *Electrical Engineering Materials*, Prentice-Hall of India Pvt. Ltd., India, (1973) 124.
15. Rajkumar K V, Rao B P C, Sasi B, Anish Kumar, Jayakumar T, Baldev Raj and Ray K K, *Mater. Sci. Eng. A,* **464** (2007) 233.
16. Hagemaier D J, *Mater. Eval.,* **30**(12) (1972) 268.
17. Rosen A, Ndiv S and Bohrer M, *Mater. Eval.* **33**(6) (1975) 135.
18. Veeraraghavan D, Pilchowski L, Natarajan B and Vasudevan V K, *Acta mater.* **46**(2) (1998) 405.
19. Collins E W and Gehlen P C, *J. Phys. F: Metal Phys.* (1971) 908.
20. Rao B P C, Jayakumar T and Baldev Raj, Electromagnetic NDE techniques for material characterisation, in Ultrasonic and advance methods for non destructive testing and material characterisation, Eds. C.H. Chen, World Scientific, (2007) 245.
21. Tarin P, Fernandez A L, Simon A G, Badia J M and Piris N M, *Mater. Sci. Eng. A,* **438** (2006) 364.
22. Reddy N S, Lee C S, Kim J H and Semiatin S L, *Mater. Sci.Eng. A,* **434** (2006) 218.